(14) Marsano, E.; Carpaneto, L.; Ciferri, A. *Mol. Cryst. Liq. Cryst.* **1987**, *153*, 263.
(15) Ernst, B.; Navard, P. *Macromolecules* **1989**, *22*, 1419.
(16) Hashimoto, T.; Takebe, T.; Suehiro, S. *Polym. J.* **1986**, *18* (2), 123.
(17) Asada, T.; Muramatsu, H.; Watanabe, R.; Onogi, S. *Macromolecules* **1980**, *13*, 867.
(18) Onogi, Y.; White, J. L.; Fellers, J. F. *J. Non-Newtonian Fluid Mech.* **1980**, *7*, 121.
(19) Zachariades, A. E.; Navard, P.; Logan, J. A. *Mol. Cryst. Liq. Cryst.* **1984**, *110*, 93.
(20) Ide, Y.; Ophir, Z. *Polym. Eng. Sci.* **1983**, *23* (5), 261.
(21) Mewis, J.; Moldenaers, P. *Mol. Cryst. Liq. Cryst.* **1987**, *153*, 29.
(22) Chen, S.; Jin, Y.; Hu, S.; Xu, M. *Polym. Commun.* **1987**, *28*, 208.
(23) Pirnia, A.; Sung, C. S. P. *Macromolecules* **1988**, *21*, 2699.
(24) Marrucci, G. *Pure Appl. Chem.* **1985**, *57*, 1545.
(25) Wissbrun, K. F. *Faraday Discuss. Chem. Soc.* **1985**, *79*, Paper 13.
(26) Takebe, T.; Hashimoto, T.; Ernst, B.; Navard, P.; Stein, R. S. *J. Chem. Phys.*, in press.
(27) Samuels, R. J. *J. Polym. Sci.* **1969**, *A2* (7), 1197.
(28) Rhodes, M. B.; Stein, R. S. *J. Polym. Sci.* **1969**, *A2* (7), 1539.
(29) Hayashi, N.; Murakami, Y.; Moritan, M.; Hashimoto, T.; Kawai, H. *Polym. J.* **1973**, *4*, 560.
(30) Ernst, B.; Navard, P.; Haudin, J. M. *J. Polym. Sci., Polym. Phys. Ed.* **1988**, *26*, 211.
(31) Shiwaku, T.; Nakai, A.; Hasegawa, H.; Hashimoto, T. *Polym. Commun.* **1987**, *28*, 174.
(32) Hudson, S. D.; Thomas, E. L.; Lenz, R. W. *Mol. Cryst. Liq. Cryst.* **1988**, *153*, 63.
(33) Hashimoto, T.; Nakai, A.; Shiwaku, T.; Hasegawa, H.; Rojstacser, S.; Stein, R. S. *Macromolecules*, in press.
(34) Moldenaers, P.; Fuller, G.; Mewis, J. *Macromolecules* **1989**, *22*, 960.
(35) Kuzuu, N.; Doi, M. *J. Phys. Soc. Jpn.* **1983**, *52*, 3486. *Ibid.* **1984**, *53*, 1031.
(36) Wood, B. A.; Thomas, E. L. *Nature*, in press.
(37) Akay, G.; Leslie, F. M. *Proceedings of the IXth International Congress on Rheology*; 1984; p 495.
(38) Ide, Y.; Chung, T. S. *J. Makromol. Sci. Polym.* **1984-1985**, *B23*, 497.
(39) Chung, T. S. *Polym. Eng. Sci.* **1986**, *26*, 901.

Registry No. HPC, 9004-64-2; PBLG (homopolymer), 25014-27-1; PBLG (SRU), 25038-53-3.

Synthesis and Characterization of Poly[[*o*-(trimethylsilyl)phenyl]acetylene][1]

Toshio Masuda,* Toshiyuki Hamano, Kenji Tsuchihara, and Toshinobu Higashimura*

Department of Polymer Chemistry, Kyoto University, Kyoto 606, Japan.
Received May 2, 1989; Revised Manuscript Received September 7, 1989

ABSTRACT: [*o*-(Trimethylsilyl)phenyl]acetylene quantitatively polymerized in the presence of WCl_6–Et_3SiH (1:1), $W(CO)_6$–$h\nu$, and $MoCl_5$–Et_3SiH (1:1) catalysts in toluene or CCl_4 at 30 °C to give a new polymer having weight-average molecular weight over 1×10^6. Effects of organometallic cocatalysts, solvents, and temperature on the polymerization were studied. The product polymer possessed the structure $[-CH{=}C(C_6H_4\text{-}o\text{-}SiMe_3)-]_n$ and was amorphous. The polymer was in the form of a dark purple solid (λ_{max} 542 nm), completely dissolved in common organic solvents such as toluene and $CHCl_3$, formed a strong film by solution casting, and did not lose weight below 280 °C in air, being fairly thermally stable.

Introduction

It has recently been found that not only phenylacetylene (PA) but also ortho-substituted PA's such as (*o*-methylphenyl)acetylene[2] (*o*-MePA) and [*o*-(trifluoromethyl)phenyl]acetylene[3] (*o*-CF_3PA) polymerize with W and Mo catalysts. Quite interestingly, poly[(*o*-methylphenyl)acetylene] [poly(*o*-MePA)] and poly[[*o*-(trifluoromethyl)phenyl]acetylene] [poly(*o*-CF_3PA)] obtained have higher molecular weights than that of poly(phenylacetylene) [poly(PA)] irrespective of the steric hindrance due to the ortho substituents. Eventually poly(*o*-CF_3PA) provides a strong film by solution casting, whereas poly(PA) is too brittle to form a free-standing film.

So far, a number of substituted polyacetylenes have been synthesized by using transition-metal catalysts.[4] Among those polymers are Si-containing polyacetylenes, some of which exhibit unique properties not seen in hydrocarbon polyacetylenes. For example, poly[1-(trimethylsilyl)-1-propyne] [poly(TMSP)] shows extremely high gas permeability[5] and ethanol permselectivity in the ethanol/water pervaporation.[6]

[*o*-(Trimethylsilyl)phenyl]acetylene (*o*-Me_3SiPA) is an ortho-substituted PA and is a Si-containing acetylene as well. It is of interest to study the polymerizability of this monomer, the molecular weight of poly[[*o*-(trimethylsilyl)phenyl]acetylene] [poly(*o*-Me_3SiPA)], and properties of this novel polymer. In this paper we report on the polymerization of *o*-Me_3SiPA and on the characterization of poly(*o*-Me_3SiPA).

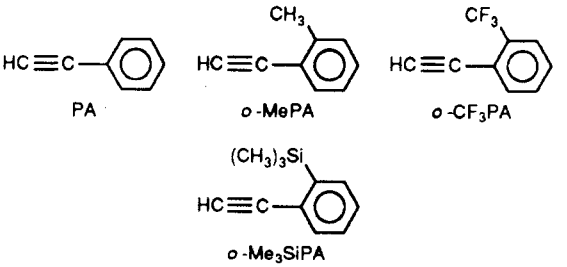

Results and Discussion

Polymerization by Various Catalysts. It has been found that mixtures of WCl_6 or $MoCl_5$ (main catalyst)

0024-9297/90/2223-1374$02.50/0

Table I
Polymerization of o-Me_3SiPA by Various Catalysts[a]

cat.	convn, %	polymer yield, %	polymer $10^{-3}\bar{M}_w$[b]	polymer $10^{-3}\bar{M}_n$[b]
WCl_6–Ph_4Sn (1:1)	100	86	1800[f]	780
$MoCl_5$–Ph_4Sn (1:1)	100	76	1600	740
$W(CO)_6$–$h\nu$[c]	100	100	3400[g]	1200
$Mo(CO)_6$–$h\nu$[c]	6	0		
$NbCl_5$[d]	100	15	1500	1100
$TaCl_5$[d]	100	3		
$[(COD)RhCl]_2$[e]	0	0		
$(Ph_3P)_2PdCl_2$	0	0		
$Fe(acac)_3$–Et_3Al (1:3)[e]	4	0		
$Ti(O\text{-}n\text{-}Bu)_4$–$Et_3Al$ (1:4)	3	0		

[a] Polymerized in toluene at 30 °C for 24 h; $[M]_0$ = 1.0 M; [transition metal] = 10 mM. [b] Determined by GPC. [c] Polymerized in CCl_4. [d] Polymerized at 80 °C. [e] Abbreviations: COD, 1,5-cyclooctadiene; acac, acetylacetonate. [f] $[\eta]$ = 1.57 dL/g (measured in toluene at 30 °C). [g] $[\eta]$ = 2.34 dL/g.

and Ph_4Sn (organometallic cocatalyst) are effective in the polymerization of substituted acetylenes.[4b] As seen in Table I, WCl_6–Ph_4Sn and $MoCl_5$–Ph_4Sn gave polymers in ca. 80% yields. The $W(CO)_6$–$h\nu$ catalyst polymerized o-Me_3SiPA quantitatively, whereas the $Mo(CO)_6$ counterpart was ineffective.

The $\bar{M}_w$ values of the polymers obtained with WCl_6–Ph_4Sn, $W(CO)_6$–$h\nu$, and $MoCl_5$–Ph_4Sn exceeded one million according to gel permeation chromatography (GPC; a polystyrene calibration used). It is especially noteworthy that the polymer formed with the $W(CO)_6$–$h\nu$ catalyst had a very high molecular weight reaching 3×10^6. The high molecular weight is supported by its large intrinsic viscosity ($[\eta]$).

In the case of group 5 transition-metal (Nb and Ta) chlorides as catalysts, the monomer was totally consumed, but methanol-insoluble polymers were formed only in small amounts. The methanol-soluble main products showed a single peak around the molecular weight of 523 corresponding to a trimer in GPC. Further, their mass spectrum showed virtually selectively three peaks of similar magnitude at 539, 540, and 541; these peaks are assignable to the NH_4^+ adduct (541) of the trimer and to those in which one or two hydrogens have been eliminated. Therefore, the oligomeric products are thought to be the cyclotrimer[1,2,4-and/or1,3,5-tris[o-(trimethylsilyl)phenyl]benzenes].

None of the group 8 transition-metal (Rh, Pd) catalysts and Ziegler-type catalysts produced any polymer from o-Me_3SiPA. The Rh and Fe catalysts are known to polymerize PA in high yield. Hence, it is inferred that, unlike W and Mo catalysts, these catalysts are very sensitive to the steric hindrance of the monomer. Consequently, the polymerization by W and Mo catalysts was examined in detail.

Polymerization by W Catalysts. Table II details the effects of organometallic cocatalysts involving group 4 and 5 main-group metals in the polymerization by WCl_6. When Et_3SiH and some other cocatalysts were used, poly(o-Me_3SiPA) was obtained quantitatively. In the case of Ph_4Sn and Ph_3SiH, the polymer yields were lower than 100% for some reason. The polymer yield was high enough even without a cocatalyst. This is consistent with the general tendency that addition of a cocatalyst mainly affects the polymerization rate for monosubstituted acetylenes, whereas a cocatalyst is usually indispensable for disubstituted acetylenes to polymerize.[4b] No large difference in the molecular weight of polymer was observed with changing the kind of cocatalyst. Et_3SiH was adopted as a cocatalyst in the following experiments.

Table II
Cocatalyst Effects on the Polymerization of o-Me_3SiPA by WCl_6[a]

no.	cocat.	convn, %	polymer yield, %	polymer $10^{-3}\bar{M}_w$[b]	polymer $10^{-3}\bar{M}_n$[b]
1	none	100	91	1500	670
2	Et_3SiH	100	100	1600[c]	670
3	Ph_3SiH	100	91	1500	720
4	$n\text{-}Bu_4Sn$	100	100	1500	640
5	Ph_4Sn	100	86	1800	780
6	Ph_3Sb	100	100	1400	510
7	Ph_3Bi	100	100	1500	710

[a] Polymerized in toluene at 30 °C for 24 h; $[M]_0$ = 1.0 M; $[WCl_6]$ = [cocat.] = 10 mM. [b] Determined by GPC. [c] $[\eta]$ = 1.57 dL/g.

Table III
Solvent Effects on the Polymerization of o-Me_3SiPA by WCl_6–Et_3SiH (1:1)[a]

solv	convn, %	polymer yield, %	polymer $10^{-3}\bar{M}_w$[b]	polymer $10^{-3}\bar{M}_n$[b]
toluene	100	100	1600	670
cyclohexane	100	100	3200	1600
CCl_4	100	100	2100	680
$(CH_2Cl)_2$	100	96	3700[c]	1900
PhOMe	100	96	1600	670
PhCOOMe	100	83	1000	390
PhCOMe	3	0		
PhCN	22	8	38	18
$PhNO_2$	0	0		

[a] Polymerized at 30 °C for 24 h; $[M]_0$ = 1.0 M; $[WCl_6]$ = 10 mM. [b] Determined by GPC. [c] $[\eta]$ = 2.39 dL/g.

The WCl_6–Et_3SiH catalyzed polymerization of the present monomer proceeded practically quantitatively in hydrocarbons, halogenated hydrocarbons, and some oxygen-containing solvents (Table III). In contrast, nitrogen-containing compounds do not appear useful as polymerization solvents. The molecular weight of polymer appreciably varied with the kind of polymerization solvents; e.g., the $\bar{M}_w$ in $(CH_2Cl)_2$ reached 3.7×10^6. It is, however, not clear at present how solvents affect the polymer molecular weight.

Figure 1a illustrates the effect of temperature on the polymerization by WCl_6–Et_3SiH in toluene. When carried out at 0 °C or above, the polymerization conversion reaches 100%. The $\bar{M}_w$ of polymer shows a maximum around 30 °C and clearly decreases with increasing temperature. Thus about 30 °C seems favorable to keep both yield and molecular weight of the polymer high.

The polymerization by WCl_6–Et_3SiH is completed in 1 h under the conditions shown in Figure 2a, being fairly rapid. The $\bar{M}_w$ of the polymer increases with polymer yield, which suggests the presence of a long-lived propagating species. The high $\bar{M}_w$ of 1.6×10^6 achieved at 1 h is maintained even if the polymerization is continued over 24 h. This indicates that polymer degradation does not occur under the polymerization conditions.

The effect of temperature on the polymerization by $W(CO)_6$–$h\nu$ is depicted in Figure 1b. This catalyst provides the polymer at 30 °C and above, being somewhat less active than WCl_6–Et_3SiH. The high $\bar{M}_w$ around 3×10^6 is achieved at relatively low temperatures such as 0 and 30 °C. As seen in Figure 2b, the polymerization by $W(CO)_6$–$h\nu$ reaches 100% in 1 h under the standard conditions. The $\bar{M}_w$ of the polymer increases with polymer yield also in this case to reach 3×10^6 finally.

Polymerization by Mo Catalysts. As seen in Table IV, the polymer yield in the polymerization by $MoCl_5$ was affected by the kind of cocatalysts. For example,

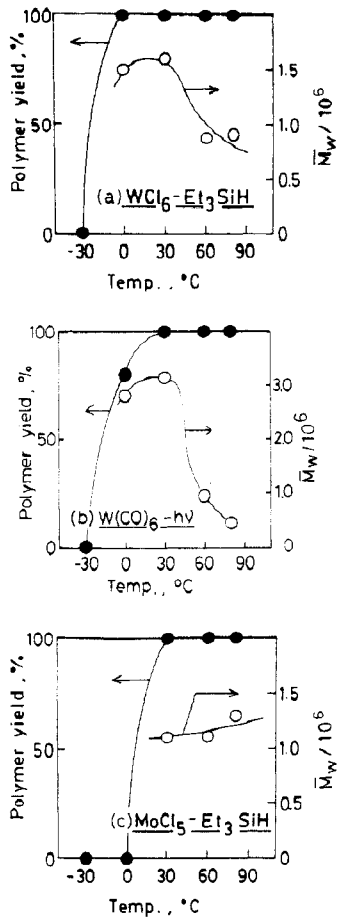

Figure 1. Temperature dependences of the polymerization of *o*-Me_3SiPA (in toluene (a, c) or in CCl_4 (b); 24 h; $[M]_0$ = 1.0 M; [cat.] = $[Et_3SiH]$ = 10 mM).

the yield was quantitative in the case of Et_3SiH, being higher than that without a cocatalyst. In contrast, Ph_3Bi exhibited an inhibiting effect. The $\bar{M}_w$ of the polymer also varied to some extent with the kind of cocatalysts. The $MoCl_5$–Et_3SiH catalyst was employed in the following experiments for the sake of comparison with the WCl_6–Et_3SiH catalyst.

Solvent effects on the polymerization by $MoCl_5$–Et_3SiH resembled those found in the polymerization by WCl_6–Et_3SiH (see Tables III and V). Namely, high polymer yields were attained in hydrocarbons, halogenated hydrocarbons, and some oxygen-containing solvents.

Regarding the polymerization temperature, the polymer yield with $MoCl_5$–Et_3SiH reaches 100% at 30 °C and above (Figure 1c). The $\bar{M}_w$ of the polymer hardly changes in the range 30–90 °C. The polymerization by $MoCl_5$–Et_3SiH at 30 °C is completed in ca. 4 h. The $\bar{M}_w$ of the polymer increases virtually in proportion to polymer yield to reach 1.1×10^6 at 100% yield (Figure 2c). Comparison of Figures 1a and 2a with Figures 1c and 2c leads to the conclusion that WCl_6–Et_3SiH is a more active catalyst for the present monomer than $MoCl_5$–Et_3SiH is.

Comparison of Polymerizations of PA's. PA polymerizes in high yield with W catalysts but does not polymerize in as high a yield with Mo catalysts (yields are lower than 50% even under optimal conditions).[4b] The polymerization behavior of 1-hexyne is similar. In contrast, *o*-Me_3SiPA, *o*-CF_3PA, and *tert*-butylacetylene polymerize quantitatively with both W and Mo catalysts. Though the reason is not clear, it is of interest that these sterically crowded monosubstituted acetylenes achieve high yields of the polymer with Mo catalysts.

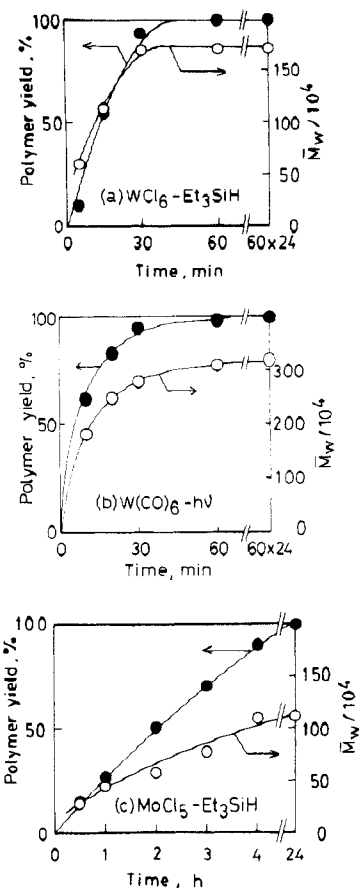

Figure 2. Time courses of the polymerization of *o*-Me_3SiPA (in toluene (a, c) or in CCl_4 (b); 30 °C; $[M]_0$ = 1.0 M; [cat.] = $[Et_3SiH]$ = 10 mM).

Table IV
Cocatalyst Effects on the Polymerization of *o*-Me_3SiPA by $MoCl_5$[a]

cocat.	convn, %	polymer yield, %	polymer $10^{-3}\bar{M}_w$[b]	polymer $10^{-3}\bar{M}_n$[b]
none	100	86	1700	780
Et_3SiH	100	100	1100[c]	470
Ph_3SiH	100	100	2600	1200
n-Bu_4Sn	100	100	570	220
Ph_4Sn	100	76	1600	740
Ph_3Sb	100	85	840	340
Ph_3Bi	28	0		

[a] Polymerized in toluene at 30 °C for 24 h; $[M]_0$ = 1.0 M; $[MoCl_5]$ = [cocat.] = 10 mM. [b] Determined by GPC. [c] $[\eta]$ = 1.16 dL/g.

Not only *o*-CF_3PA but also *o*-Me_3SiPA give a polymer whose $\bar{M}_w$ exceeded one million. The $\bar{M}_w$ of poly(PA) is no more than 2×10^5 at the highest and that of poly(*o*-MePA) is in between. Thus the bulkiness of the substituent in an acetylenic monomer is a very important factor in determining the molecular weight of the polymer formed. The fact that both *o*-Me_3SiPA and *o*-CF_3PA can give high molecular weight polymers implies that the electronic effect of substituent is not a substantial factor for the high molecular weight.

In order to gain knowledge on the relative reactivity of monomers, copolymerizations of *o*-Me_3SiPA with PA and *o*-CF_3PA were studied in toluene at 30 °C ($[M_1]_0$ = $[M_2]_0$ = 0.50 M; $[WCl_6]$ = 10 mM). The relative reactivities of PA, *o*-Me_3SiPA, and *o*-CF_3PA, which were determined from their relative initial polymerization rates, were 6.2, 1.0, and 0.50, respectively. Thus, PA is most reactive among these monomers, while *o*-Me_3SiPA and

Table V
Solvent Effects on the Polymerization of o-Me_3SiPA by $MoCl_5$–Et_3SiH (1:1)[a]

solvent	convn, %	polymer yield, %	polymer $10^{-3}\bar{M}_w$[b]	polymer $10^{-3}\bar{M}_n$[b]
toluene	100	100	1100	470
cyclohexane	80	76	370	49
CCl_4	100	100	820	190
$(CH_2Cl)_2$	100	87	2300[c]	1100
PhOMe	100	93	1300	460
PhCOOMe	100	87	680	290
PhCOMe	15	0		
PhCN	10	0		
$PhNO_2$	8	0		

[a] Polymerized at 30 °C, for 24 h; $[M]_0$ = 1.0 M; $[MoCl_5]$ = 10 mM. [b] Determined by GPC. [c] $[\eta]$ = 1.69 dL/g.

o-CF_3PA show similar reactivities in the copolymerization. This agrees with previous results that a bulkier acetylene is less reactive in copolymerization because of its weaker coordinating ability to the propagating species.[7] It is noteworthy that the reactivities of o-Me_3SiPA and o-CF_3PA are close to each other, irrespective of the opposite electronic effects of the ortho substituents.

Polymer Structure. The structure of poly(o-Me_3SiPA) did not depend on the polymerization conditions. Hence, the data of the polymer sample from Table II, number 2, will be described.

The combustion analytical data of poly(o-Me_3SiPA) are as follows. Calcd for $(C_{11}H_{14}Si)_n$: C, 75.79; H, 8.09; Si, 16.12. Found: C, 75.78; H, 8.18; Si, 16.81. Thus the polymer possesses just the elemental composition for the polymerization product.

While strong ≡C—H (3290 cm^{-1}) and weak C≡C (2100 cm^{-1}) absorptions are observed in the IR spectrum of the monomer, these bands disappear in the polymer (Figure 3a). Strong absorptions characteristic of the SiC–H and Si–C bonds are seen in both the monomer and the polymer.

In the ^1H NMR spectrum of poly(o-Me_3SiPA) appears a broad signal due to the olefinic and aromatic protons (δ 8.0–4.5) and a sharp one due to the methyl protons (δ 0.0); the acetylenic proton in the monomer (δ 3.2) and any other unexpected protons are not seen (Figure 3b). The ^{13}C NMR spectrum of polymer exhibits signals of sp^2 carbons (δ 150–125) and of methyl carbons (δ 1); cf. sp carbons in the monomer: δ 80.9 and 85.9. The ^{13}C NMR data corresponds well to ^1H NMR data (Figure 3c).

The IR and NMR spectra above support the idea that the polymer possesses alternating double bonds in the main chain as shown in Figure 3. The polymer should have the regular head-to-tail structure because the head-to-head structure seems difficult to form. The geometric structure of the main chain, however, remains unsolved.

In general, the UV–visible spectrum of a substituted polyacetylene gives some information about the conformation. Quite interestingly, poly(o-Me_3SiPA) shows a fairly large absorption maximum (ϵ_{max} 6400 M^{-1} cm^{-1}) in a very long wavelength region (λ_{max} 542 nm) (see Figure 4). The absorption extends up to ca. 700 nm. The absorption maximum of poly(o-CF_3PA) is at 458 nm, being relatively near that of poly(o-Me_3SiPA), while that of poly(PA) is below 300 nm.[3b] In contrast, most disubstituted acetylene polymers exhibit absorptions only in the UV region.[4b] The reason why ortho substituents in poly(PA) cause a red shift is, however, not clear at present.

The X-ray diffraction data of poly(o-Me_3SiPA) obtained with Cu Kα radiation is as follows [2θ (Δ2θ/2θ)]: 7.6° (0.368); 15.1° (0.219); 23.3° (0.202). As seen from the ratios of half-height width to diffraction angle (Δ2θ/2θ > 0.20), the peaks are rather broad; this indicates that the present polymer is amorphous. The 2θ values are in a ratio of 1:2:3, being attributed to the first-, second-, and third-order diffractions, respectively,[1] in the Bragg

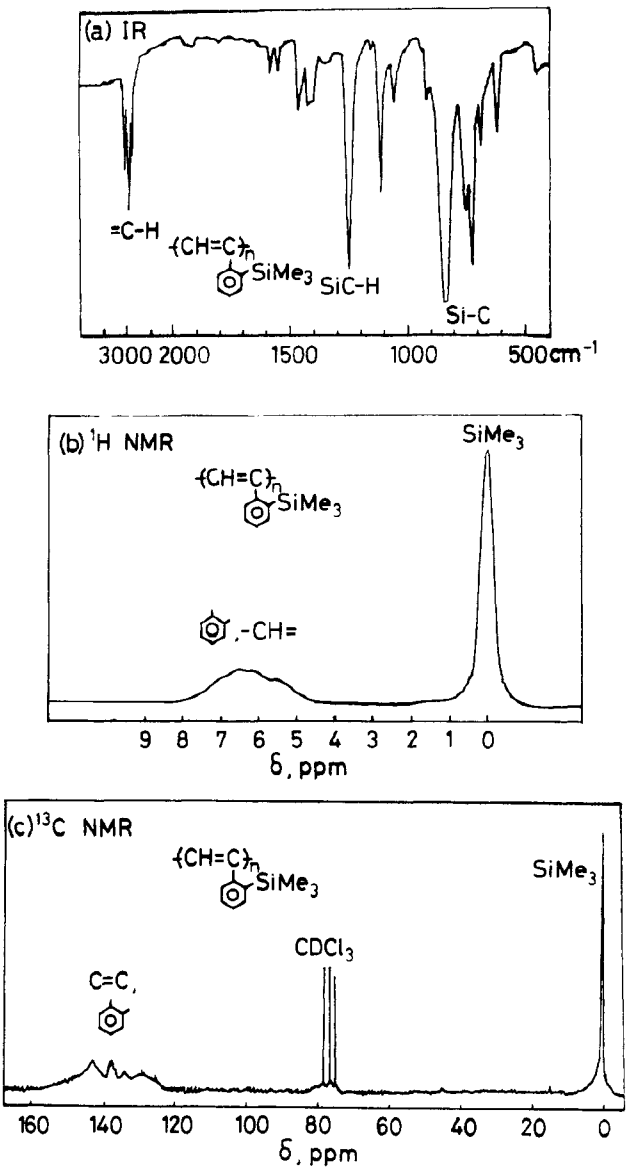

Figure 3. IR, ^1H NMR, and ^{13}C NMR spectra of poly(o-Me_3SiPA) (sample from Table II, number 2; IR, KBr pellet; NMR $CDCl_3$ solution).

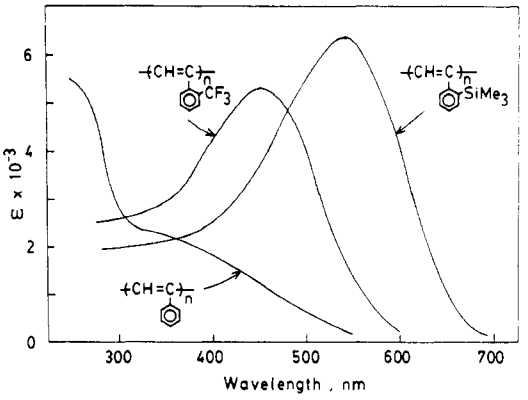

Figure 4. UV–visible spectra of poly(o-Me_3SiPA) and related polymers [poly(o-Me_3SiPA) sample from Table II, number 2, measured in THF; other data from ref 3b].

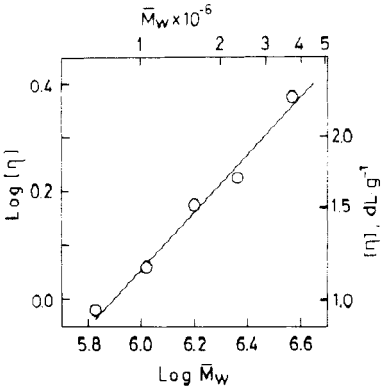

Figure 5. $[\eta]$ vs $\bar{M}_w$ plot for poly(*o*-Me_3SiPA) (the samples with polydispersity ratio of around 2.5 were used; $[\eta]$ measured in toluene at 30 °C, and $\bar{M}_w$ determined by GPC).

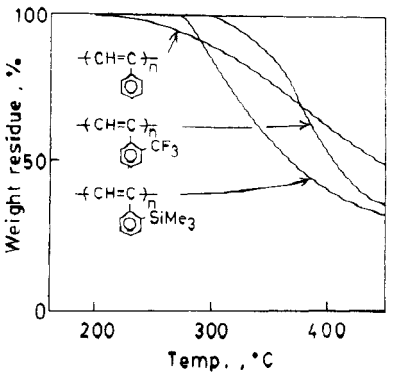

Figure 6. TGA curves of poly(*o*-Me_3SiPA) and related polymers [poly(*o*-Me_3SiPA) sample from Table II, number 2, measured in air at a heating rate of 10 °C/min; other data from ref 3b and 8].

equation. The 2θ of 7.6° corresponds to the distance of 1.16 nm, suggesting the presence of a certain regular structure within a short range.

Polymer Properties. There were no discernible differences in the properties of poly(*o*-Me_3SiPA) with polymerization conditions. The following properties are of the polymer obtained with WCl_6–Et_3SiH (Table II, number 2).

Poly(*o*-Me_3SiPA) has the form of dark purple solid irrespective of the polymerization conditions. Poly(*o*-CF_3PA) is a dark brown solid, while poly(PA) is brown (W catalysts) or yellow (Mo catalysts). Therefore, it can be said that the ortho-substituted poly(PA)s are more deeply colored than poly(PA).

Poly(*o*-Me_3SiPA) dissolved in benzene, toluene, cyclohexane, CCl_4, $CHCl_3$, CH_2Cl_2, tetrahydrofuran, and triethylamine and partly dissolved in chlorobenzene, anisole, $(CH_2Cl)_2$, and diethyl ether. Its nonsolvents include hexane, heptane, 1,4-dioxane, acetone, acetophenone, ethyl acetate, methyl benzoate, nitrobenzene, *N*,*N*-dimethylformamide, and acetonitrile. These solubility properties resemble those of poly(PA) and poly(*o*-CF_3PA).

A logarithmic plot of the intrinsic viscosity vs $\bar{M}_w$ of poly(*o*-Me_3SiPA) is shown in Figure 5. The plot can be represented by a good linear relationship, leading to the following equation:

$$[\eta] = K\bar{M}_w^{\,a} \quad (K = 2.42 \times 10^{-5}\ \mathrm{dL \cdot g^{-1}};\ a = 0.764)$$

The exponent a is 0.76 being close to that of poly(*o*-CF_3PA) ($a = 0.59$).[3a] These values are not so large as those for disubstituted acetylene polymers [e.g., poly(TMSP), $a = 1.04$; $(-CCl{=}CPh-)_n$, $a = 1.07$].[4b] Apparently these monosubstituted acetylene polymers assume less expanded conformations in solution than do disubstituted acetylene polymers.

One can prepare a strong, free-standing film by casting poly(*o*-Me_3SiPA) from toluene solution as in the case of poly(*o*-CF_3PA). In contrast, poly(PA) is too brittle to form a film, and the film from poly(*o*-MePA) is rather brittle. The film-forming properties of poly(*o*-Me_3SiPA) and poly(*o*-CF_3PA) are attributable to their high molecular weight. We believe that the ease of preparation of poly(*o*-Me_3SiPA) film will greatly help find practical applications in the future.

Poly(*o*-Me_3SiPA) began to lose weight at about 280 °C in thermogravimetric analysis (TGA) in air (Figure 6). This temperature is higher than that for poly(PA) and is close to that for poly(*o*-CF_3PA). Further, the thermal stability of a polymer can be evaluated by the α value, which is the probability of main-chain scission on heat treatment in air at 120 °C for 20 h (defined as follows):[8]

$$\alpha = \frac{1}{\overline{DP}_n} - \frac{1}{\overline{DP}_{n,o}}$$

Here $\overline{DP}_n$ and $\overline{DP}_{n,o}$ are the number-average degrees of polymerization after and before the heat treatment. The α values are as follows: poly(*o*-Me_3SiPA), 2.0×10^{-4}; poly(*o*-CF_3PA),[3b] 2.5×10^{-3}; poly(PA),[8] 1.6×10^{-2}. These ortho-substituted poly(PA)s do not suffer any molecular weight decrease or oxidation even after they have been left in air at room temperature over a few months, while poly(PA) gradually undergoes a molecular weight decrease and is oxidized to some extent. Thus the ortho substituents are clearly effective in enhancing the stability of the poly(PA).

The tensile properties of poly(*o*-Me_3SiPA) at 25 °C are as follows:[9] Young's modulus, 700 MPa; tensile strength, 23 MPa; elongation at break, 4.3%. Thus it is a hard and brittle polymer. The glass transition temperature observed by dynamic viscoelasticity is above 200 °C.[9] The softening point was around 360 °C.

The electrical conductivity of poly(*o*-Me_3SiPA) at 25 °C was 4×10^{-15} $S \cdot cm^{-1}$; i.e., it is a typical insulator like poly(PA) and poly(*o*-CF_3PA). The ESR spectrum in the solid state at 25 °C showed a singlet peak with a line width of 8.1 G and a g value of 2.0034; the unpaired-electron density was 7.3×10^{17} spin/g. The unpaired-electron densities (25 °C) of poly(PA) and poly(*o*-CF_3PA) (W catalyst) are 7.9×10^{16} and 6.1×10^{17} spin/g, respectively;[3b,4b] that is, the value for poly(PA) is rather smaller. The high stability of these ortho-substituted poly(PA)s may be because it is difficult for oxygen to attack the main chain owing to the steric effect.

The oxygen permeability coefficient (P_{O_2}) of the present polymer at 25 °C is 78 barrers [1 barrer = 1×10^{-10} cm^3 (STP)·cm·cm^{-2}·s^{-1}·$cmHg^{-1}$], and the separation factor against nitrogen (P_{O_2}/P_{N_2}) is 3.3.[5b] This P_{O_2} value is about 1/5 that of poly(dimethylsiloxane), being very large among those of glassy polymers.

Concluding Remarks

Poly(*o*-Me_3SiPA), a new, high-molecular-weight polymer ($\bar{M}_w \sim 1 \times 10^6$) is produced with W and Mo catalysts. Since the monomer is readily prepared through one-pot reactions from PA, it can be said that the access to the present polymer is very easy. Basic properties of the polymer have been elucidated in the present study. Among substituted polyacetylenes, this polymer has many salient features, such as deep color, good air-stability, and film-forming property. The gas permeability,[5b]

photoconductivity,[10] and electrochromism[11] of poly(o-Me_3SiPA) have recently been reported elsewhere. We hope that novel functions will be developed further with use of the present polymer.

Experimental Section

Materials. The monomer was prepared according to the following scheme with some modifications of the method of Brandsma:[12]

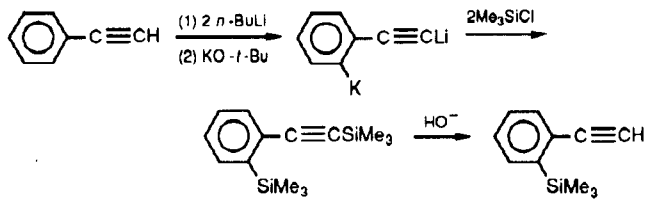

A 1-L, three-necked, round-bottomed flask was equipped with a reflux condenser, a three-way stopcock, a pressure-equalizing dropping funnel, and a magnetic stirring bar. The flask was flushed with dry nitrogen, and the subsequent procedures for the silylation reaction were carried out under a dry nitrogen atmosphere. A hexane solution of *n*-butyllithium (265 mL, 1.6 M, 0.42 mol) was placed in the flask with a syringe, and the hexane (ca. 150 mL) was evaporated with an aspirator under magnetic stirring. After the flask was cooled at −20 °C, tetrahydrofuran (THF; 100 mL; dried over sodium) was gradually added. At the same temperature, a solution of PA (22 mL, 0.20 mol; distilled) in THF (50 mL) was added dropwise and left for 1 h. The dark red reaction mixture was cooled to −65 °C, and a solution of potassium *tert*-butoxide (27 g, 0.24 mol) in THF (200 mL) was added dropwise, and the dark purple mixture was stirred at −10 °C for 1 h. Then chlorotrimethylsilane (53 mL, 0.42 mol; distilled) was gradually added at −50 °C, and the pale yellow mixture was allowed to stand at room temperature overnight. Hexane and THF were evaporated with a rotary evaporator. A solution of potassium hydroxide (30 g) in 95% ethanol (400 mL) was added to the white reaction mixture, and the flask was heated at 80 °C. The alkyne desilylation reaction was monitored by gas chromatography (GC) and shown to be completed within 1 h. Then ice water (500 mL) was added. The product was extracted with diethyl ether, washed with water, and dried over anhydrous magnesium sulfate overnight. Diethyl ether was evaporated, and the product was distilled twice at reduced pressure from calcium hydride: bp 85 °C (10 mmHg) [lit.[12a] 85 °C (10 mmHg)]; yield 75%; purity >99% (by GC); d_4^{20} 0.883.

Transition-metal compounds and organometallic cocatalysts were all commercially obtained and used without further purification with care being taken not to be decomposed by moisture and/or air. Polymerization solvents were purified by the standard methods.

Polymerization. The polymerization procedure for Table II, number 2, is described below as a typical example. The procedure was performed under dry nitrogen throughout.

A monomer solution (4.2 mL) was prepared in a Schlenk tube by mixing the monomer (2.07 mL, 1.83 g, 10.5 mmol), bromobenzene (0.50 mL, internal standard of GC), and toluene (1.63 mL). Another Schlenk tube was charged with WCl_6 (38.6 mg, 0.10 mmol), Et_3SiH (15.9 μL, 11.6 mg, 0.10 mmol), and toluene (6.0 mL); this catalyst solution was aged at 30 °C for 15 min. Then 4.0 mL of the monomer solution was added to the catalyst solution. Polymerization was carried out at 30 °C for 24 h and was terminated with a toluene/methanol (volume ratio 4:1) mixture (1 mL); the very viscous solution was diluted with toluene (30 mL). After determination of monomer conversion by GC (PEG6000 3 m, 145 °C), the polymerization mixture was further diluted with toluene (120 mL) and was poured into methanol (2 L) under stirring to precipitate the polymer formed. Then the polymer was filtered and dried. The polymer yield was determined by gravimetry.

In the case of $W(CO)_6$–$h\nu$ and $Mo(CO)_6$–$h\nu$ catalysts, catalyst solutions were prepared by irradiation of CCl_4 solution of $W(CO)_6$ or $Mo(CO)_6$ with a 400-W high-pressure Hg lamp from a 5-cm distance at 30 °C for 30 min.

Characterization. Molecular weights of polymers were determined by GPC with use of a polystyrene calibration. GPC curves were observed with a Jasco Trirotar liquid chromatograph [eluent, $CHCl_3$; columns, Shodex A805, A806, and A807 polystyrene gels (Showa Denko, Co., Jpn)]. Monodisperse polystyrene samples with $\bar{M}_n$'s of 1.1×10^5, 3.0×10^5, 6.5×10^5, 1.8×10^6, 2.0×10^6, 3.8×10^6, 6.8×10^6, and 2.0×10^7 were used to make a calibration curve. A liquid chromatograph equipped with columns of Shodex A802, A803, and A804 was used for the analysis of oligomeric products.

The GPC peaks of the polymers had a common shape, sharp on the low-molecular-weight side and gentle on the high-molecular-weight side. Since the leadings on the high-molecular-weight side were partly out of the calibration limit, the $\bar{M}_w$ and $\bar{M}_n$ values are not very accurate. Especially at a very dilute concentration of polymer sample (e.g., 0.3 g/dL), the GPC peak shifted to the high-molecular-weight side, and the leading on the high-molecular-weight side was quite pronounced. This might be due to a polymer-electrolyte-like property resulting from the doping by some impurities. This was not a case at high concentrations (1.5–3.0 g/dL), at which almost all the measurements were carried out.

Intrinsic viscosities ([η]) of polymers were measured in toluene at 30 °C by using a Ubbelohde-type viscometer in the concentration range 0.1–0.4 g/dL. The plots of η_{sp}/c vs c were all linear.

Mass spectra were observed with a Shimadzu QP-1000 mass spectrometer equipped with a thermospray unit (Vestec, Model 750B). Sample solutions were prepared by dissolving samples (~0.5 mM) and ammonium acetate (0.1 M) in methanol, and the solutions (20 μL) were injected into the thermospray unit. Then the samples were chemically ionized with the aid of an electron beam of 200 eV.

NMR spectra were measured on a JEOL FX90Q spectrometer. IR spectra and UV–visible spectra were recorded with Shimadzu IR435 and UV190 spectrophotometers. Other analyses were carried out as described before.[2,3b]

Acknowledgment. We thank Dr. T. Hashimoto and K. Saijo (Kyoto University) for the measurement of X-ray diffraction and Dr. T. Kawamura (Gifu University) for the measurement of ESR. This research was partly supported by the Grant-in-Aid for Scientific Research on Priority Areas "New Functionality Materials—Design, Preparation and Control" from the Ministry of Education, Science and Culture, Japan (No. 63604560).

References and Notes

(1) Part 10 of "Polymerization of Si-Containing Acetylenes". Part 9: Masuda, T.; Tsuchihara, K.; Ohmameuda, K.; Higashimura, T. *Macromolecules* **1989**, *22*, 1036.

(2) Abe, Y.; Masuda, T.; Higashimura, T. *J. Polym. Sci., Polym. Chem. Ed.* **1989**, *27*, 4267.

(3) (a) Muramatsu, H.; Ueda, T.; Ito, K. *Macromolecules* **1985**, *18*, 1634. (b) Masuda, T.; Hamano, T.; Higashimura, T.; Ueda, T.; Muramatsu, H. *Macromolecules* **1988**, *21*, 281.

(4) For reviews, see: (a) Gibson, H. A. In *Handbook of Conducting Polymers*, Skotheim, T. A., Ed.; Marcel Dekker: New York, 1986; Vol. I, Chapter 11. (b) Masuda, T.; Higashimura, T. *Adv. Polym. Sci.* **1986**, *81*, 121.

(5) Recent relating articles: (a) Ichiraku, Y.; Stern, S.; Nakagawa, T. *J. Membr. Sci.* **1987**, *34*, 5. (b) Masuda, T.; Iguchi, Y.; Tang, B.-Z.; Higashimura, T. *Polymer* **1988**, *29*, 2041.

(6) (a) Masuda, T.; Takatsuka, M.; Tang, B.-Z.; Higashimura, T. *J. Membr. Sci.*, in press. (b) Masuda, T.; Tang, B.-Z.; Higashimura, T. *Polym. J.* **1986**, *18*, 565. (c) Ishihara, K.; Nagase, Y.; Matsui, K. *Makromol. Chem., Rapid Commun.* **1986**, *7*, 43.

(7) (a) Masuda, T.; Yoshizawa, T.; Okano, Y.; Higashimura, T. *Polymer* **1984**, *25*, 503. (b) Hamano, T.; Masuda, T.; Higashimura, T. *J. Polym. Sci., Polym. Chem. Ed.* **1988**, *26*, 2603.

(8) Masuda, T.; Tang, B.-Z.; Higashimura, T.; Yamaoka, H. *Macromolecules* **1985**, *18*, 2369.
(9) Masuda, T.; Matsumoto, T.; Tang, B.-Z.; Tanaka, A.; Higashimura, T., unpublished data.
(10) Kang, E. T.; Neoh, K. G.; Masuda, T.; Higashimura, T.; Yamamoto, M. *Polymer* **1989**, *30*, 1328.
(11) Fujisaka, T.; Suezaki, M.; Koremoto, T.; Inoue, T.; Masuda, T.; Higashimura, T. *Polym. Prepr. Jpn.* **1989**, *38* (3), 797.
(12) (a) Brandsma, L.; Hommes, H.; Verkruijsse, H. D.; de Jong, R. L. P. *Recl. Trav. Chim. Pays-Bas* **1985**, *104*, 226. (b) Brandsma, L.; Verkruijsse, H. D. *Synthesis of Acetylenes, Allenes and Cumulenes*; Elsevier: Amsterdam, 1981; p 85.

Registry No. PhC≡CH, 536-74-3; Me_3SiCl, 75-77-4; $Me_3SiC_6H_4$-*o*-C≡CSiMe_3, 62618-20-6; $Me_3SiC_6H_4$-*o*-C≡CH, 78905-09-6; WCl_6, 13283-01-7; (*o*-Me_3SiPA) (homopolymer), 112754-88-8; (*o*-Me_3SiPA) (SRU), 124943-12-0; Ph_4Sn, 595-90-4; $MoCl_5$, 10241-05-1; $W(CO)_6$, 14040-11-0; $NbCl_5$, 10026-12-7; Et_3SiH, 617-86-7; Ph_3SiH, 789-25-3; *n*-Bu_4Sn, 1461-25-2; Ph_3Sb, 603-36-1; Ph_3Bi, 603-33-8.

Microstructural Evolution of a Silicon Oxide Phase in a Perfluorosulfonic Acid Ionomer by an in Situ Sol–Gel Reaction. 2. Dielectric Relaxation Studies

K. A. Mauritz* and I. D. Stefanithis

Department of Polymer Science, University of Southern Mississippi, Southern Station Box 10076, Hattiesburg, Mississippi 39406-0076. *Received May 16, 1989; Revised Manuscript Received August 29, 1989*

ABSTRACT: Microcomposite membranes were produced via the in situ diffusion-controlled and acid-catalyzed sol–gel reaction for tetraethoxysilane in prehydrated and methanol-swollen Nafion perfluorosulfonic acid films. The storage and loss components of the complex dielectric constants of these modified membranes were determined over the frequency range 5 Hz to 13 MHz as a function of invasive silicon oxide content and temperature. The large storage components displayed by these microcomposites suggest the action of an interfacial polarization which, in turn, suggests the persistence of a microphase-separated, i.e. clustered, morphology after incorporation of the silicon oxide structures. Long-range motions of charge, tentatively attributed to the intercluster hopping of protons, is strongly manifest on the loss spectra. A parameter, *n*, which is extracted from the isothermal loss component vs frequency spectra, is reflective of the degree of connectivity of underlying charge pathway networks. *n* vs temperature or silicon oxide content relationships are then viewed as coarsely indicative of the evolution of the microcomposite morphological texture with the variance of these two factors. The observed range of *n* is broad, which suggests considerable morphological differentiation, and definite trends in this parameter are seen. While *n* vs filler level at constant temperature exhibits organized but complex behavior, *n* vs temperature at constant filler level plots appear as distinctly increasing curves except at the highest loading. A structural-mechanistic assignment of three absorption peaks detected beyond the dc conduction region for the microcomposites as well as for the unfilled acid precursors is not evident at this time, although the lowest frequency peak might be due to the relaxation of polarization across clusters.

Introduction

Mauritz et al. have recently reported on the formulation of unique microcomposite membranes via the in situ growth of a dispersed silicon oxide phase in Nafion[1] perfluorosulfonic acid films.[2,3] In short, an acid-catalyzed, diffusion-controlled, sol–gel reaction for tetraethoxysilane (TEOS) was affected in prehydrated and alcohol-swollen membranes that were immersed in TEOS/alcohol solutions for various times after which the membranes were dried and annealed in controlled fashion to optimize the cross-linking of the in situ gel network. It was initially hypothesized and is now becoming increasingly clear that the final morphology of the invasive inorganic phase is ordered by the original polar/nonpolar phase-separated morphology presented by the perfluorosulfonic acid matrix.

Our previous FT-IR, ^{29}Si NMR, and mechanical tensile studies portray an internal silicon oxide network structure that is rather heterogeneous on a molecular scale, being increasingly less interconnected but more strained with increasing gel content. While it appears that silicon oxide clusters initially grow in single isolation, it was suggested that a percolation threshold is eventually reached at which the clusters become interknitted by $(\equiv SiO)_n$ chains over macroscopic dimensions.

In this work, we report results of the characterization of these hybrid materials by means of dielectric relaxation spectroscopy. We had previously investigated the nature of short- and long-range ion motions and their relationship to the ion-clustered morphology in identical Nafion perfluorosulfonate membranes imbibed with a variety of aqueous electrolytes over ranges of concentration and temperature.[4-7] The mechanistic concepts that have emerged from our investigations of these systems have provided valuable insight for the interpretation of the similar dielectric relaxation spectra reported for the closely related silicon oxide-filled Nafion systems in this work.

In general terms, compositional segregation or phase separation with controlled interfacial geometry presents an opportunity to design materials with interesting dielectric or charge transport properties that are not possible with microstructurally homogeneous materials. Owing to considerable differences in electrical polarizabilities

0024-9297/90/2223-1380$02.50/0